Effect of Infill Patterns on Heating for Additively Manufactured Compression Molds

Seokpum Kim[1], Pritesh Yeole[1,2,4], Ahmed Arabi Hassen[3], Vipin Kumar[3], Vlastimil Kunc[1], Uday Vaidya[1,2,4,*]

1. Energy and Transportation Science Division, Oak Ridge National Laboratory, Oak Ridge, TN 37830, USA
2. Department of Mechanical, Aerospace, and Biomedical Engineering, University of Tennessee, Estabrook Rd, Knoxville, TN 37996, USA
3. Materials Science and Technology Division, Oak Ridge National Laboratory, Oak Ridge, TN 37830, USA
4. Institute for Advanced Composites Manufacturing Innovation (IACMI), 2370 Cherahala Blvd, Knoxville TN 37932, USA

* Corresponding Author

E-mail: uvaidya@utk.edu, Tel: +1-865-974-7620

ABSTRACT

Carbon Fiber Reinforced Polymer (CFRP) composites have been used in additive manufacturing (AM) to increase the stiffness and strength of the parts. CFRP produced by AM is being considered for tooling applications. In AM, short carbon fibers are aligned along the deposition direction. However, it results in anisotropic thermal properties that affect the heat transfer and warpage of the final part. In this study, three male molds with different infill patterns were considered based on the slicing software for the extrusion deposition fabrication-additive manufacturing (EDF-AM) process. These include (a) 0°: infill pattern along the printing direction; (b) 90°: infill pattern perpendicular to the printing direction; (c) 0°/90°: alternate layers along and perpendicular directions. Finite Element Analysis (FEA) was conducted to understand the effect of infill pattern on a heat propagation. The results show that the directionality of the infill affects the heating performance.

This manuscript has been authored by UT-Battelle, LLC under Contract No. DE-AC05-00OR22725 with the U.S. Department of Energy. The United States Government retains and the publisher, by accepting the article for publication, acknowledges that the United States Government retains a non-exclusive, paid-up, irrevocable, worldwide license to publish or reproduce the published form of this manuscript, or allow others to do so, for United States Government purposes. The Department of Energy will provide public access to these results of federally sponsored research in accordance with the DOE Public Access Plan (http://energy.gov/downloads/doe-public-access-plan).

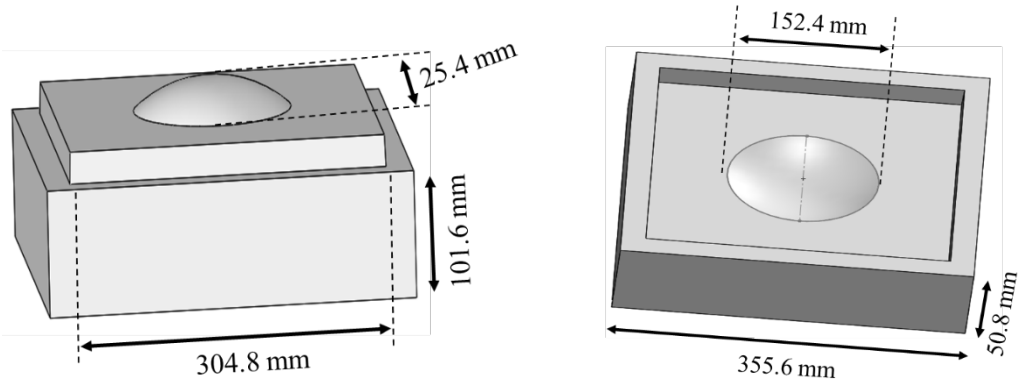
1. INTRODUCTION

The extrusion deposition fabrication – additive manufacturing (EDF-AM) system at Oak Ridge National Laboratory includes a single screw extruder in which the screw rotates inside a heated barrel and a molten material is extruded out from the deposition nozzle under high pressure [1]. Short carbon fibers in the extruded material are highly aligned along the deposition direction, and therefore, the thermal conductivity of a carbon fiber printed component is anisotropic [2]. Specifically, the extruded bead has higher conductivity in printing direction (deposition direction, or X direction) than the conductivity in the other two perpendicular directions (Y- and Z-directions). The anisotropy can be utilized to improve the performance of an AM produced part by combining the design and deposition direction control. The flexibility of the EDF-AM process allows precise control of the deposition direction (toolpath). Smith et al. [3] successfully achieve a 20% improvement in the performance of the heat sink by controlling the printing direction. Jia et al. [4] studied the specific orientation of graphite flakes to impart high through-plane thermal conductivity for maximum heat dissipation in the AM produced part. The orientation of discontinuous CFs also affects the thermal expansion of the part; expansion is more constrained along the deposition direction or fiber alignment direction due to very high thermal conductivity values of aligned CF to dissipate heat more efficiently. Deformation in the molds can lead to a significant distortion in the final parts made from these molds. Hence, maintaining a tight tolerance even at high working temperature is one of the most critical challenges with AM molds. Several studies were conducted on AM tools for high-temperature applications and promising results were obtained, where tool deformations stayed within acceptable limits [5, 6].

This work investigates the relationship between print orientation (deposition path), and part thermal performance made of 50% by weight carbon fiber reinforced polyphenylene sulfide composite pellets (50CF-PPS). A computational prediction of heat transfer is demonstrated in this study, based on the toolpaths generated from three different infill patterns. A multi-step approach is followed in the present work as (1) anisotropic thermal conductivity of the extruded bead (2) toolpath based on the infill pattern of the molds (determined by slicing software). This research concerns the different infill patterns and their effect on the heat transfer in composite molds manufactured by the EDF-AM process.

2. MATERIALS AND SAMPLE PREPARATION

In this study, 50CF-PPS was selected because PPS is a semi-crystalline thermoplastic polymer with a high heat deflection temperature [7]. The melting point of PPS is 285 °C. In this research, a mold, as shown in Figure 1, was manufactured. The infill pattern is the interior structure/geometry of the printed cross-section. Infill density and geometric patterns have a significant effect on the mechanical performance [8]. In BAAM printing, fibers are aligned along the deposition direction. Therefore, the structure of the infill pattern has a significant influence on the fiber orientation, which has a simultaneous effect on the thermal conductivity and the warpage of the final part. To understand the effect of infill pattern, three molds of the same geometry containing an infill pattern of 0° (along the deposition direction), 90° (transverse to the deposition direction) and 0°/90° (one layer along the deposition direction while the second transverse) were prepared. The outside perimeter with 3 layers was kept constant. The schematic of various infill patterns is shown in Figure 2.



(a) (b)

Figure 1: Dome-shaped AM printed Mold (a) Male Mold (b) Female Mold

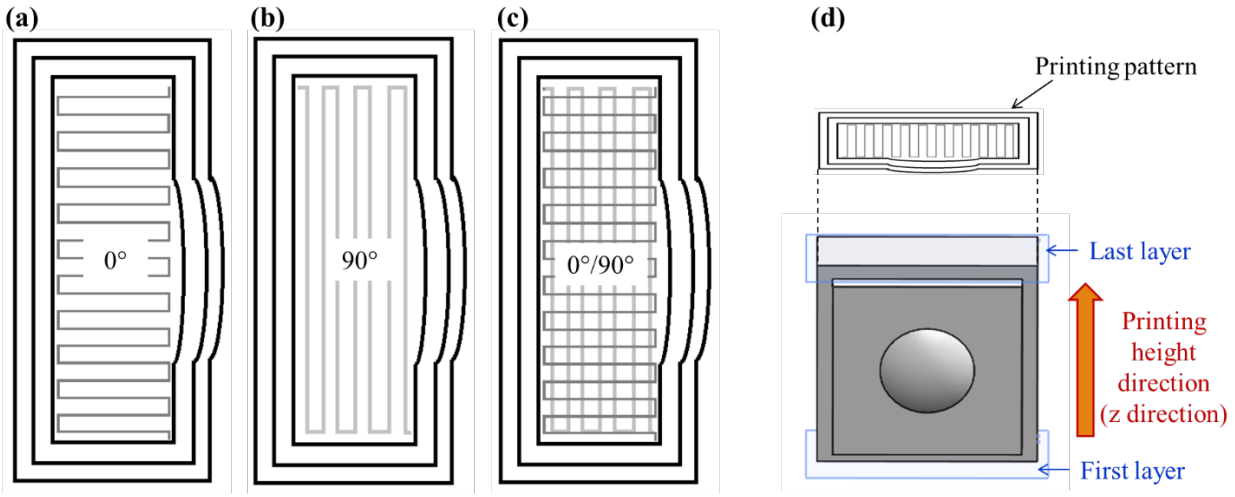


Figure 2: Infill Pattern (a) 0° (b) 90° (c) 0°/90°. The bead width: 13.97 mm (0.55”), bead height: 5.08 mm (0.2”), and infill overlap: 10% - 15% (d) Printing direction

In AM FRC samples, it is expected to have different thermal conductivity along with the three principal directions due to the fiber orientation: X-direction – parallel to the motion of extruder, Z-direction – interlayer direction, Y-direction – perpendicular to both extruder and interlayer direction. In this study, the transient plane source (TPS) technique [9] was used to measure the thermal conductivity of the samples. The BAAM screw extruder has five heating zones to melt the polymer; zone 1: 305 °C, zone 2: 321 °C, zone 3: 326 °C, zone 4: 337 °C, zone (tip): 337 °C. A block of 304.8 mm × 304.8 mm ×304.8 mm was printed with a unidirectional orientation of the deposited beads, and a smaller cube of 50.8 mm^3 was extracted from it for thermal conductivity measurement. The experimental procedure, results, and discussion of thermal conductivity measurement of 50CF-PPS are explained in Ref. [10].

3. THERMAL CONDUCTIVITY MEASUREMENT

Table 1: Thermal conductivity data at various temperatures

Sr. No.	Temperature (°C)	Thermal Conductivity (W/m K)		
		X-Direction	Z-Direction	Y-Direction
1	23	1.403 ± 0.040	0.397 ± 0.005	1.290 ± 0.017
2	58	1.479 ± 0.017	0.474 ± 0.004	1.239 ± 0.022
3	99	1.488 ±0.026	0.463 ± 0.009	1.349 ± 0.009
4	123	1.485 ± 0.040	0.445 ± 0.004	1.289 ± 0.061
5	159	1.498 ± 0.007	0.466 ± 0.006	1.267 ± 0.010

Thermal conductivity of 50CF-PPS samples was measured in the temperature range from room temperature to 170 °C, and it was observed that the thermal conductivity at any given temperature in X-direction was higher when compared to Y-direction and Z-direction. As explained in the previous section, CF tends to align in the deposition direction of BAAM extruder representing higher thermal conductivity. A tampering system was used in order to increase the bonding between deposited layers (Z- direction). During tampering, material partially squeezed out in Y-direction and forced some of the chopped fibers to align in Y-direction. Thus, it can be estimated that the thermal conductivity of BAAM printed samples in Y-direction was in between X-direction and Z-direction. Thermal conductivity values are given in Table 1.

4. FINITE ELEMENT ANALYSIS

Finite Element Analysis (FEA) was performed on the male molds with three different infill geometries, as shown in Fig. 2. A commercial FEA tool, ABAQUS 2018, was used for computational thermal analysis. The geometric model is discretized into 28.6k elements, including 13.8k tetrahedron elements and 14.8k hexahedron elements. The element size in the z-direction is 5.08 mm, which is the same as the layer height (= slicing thickness) of the 3D-printed mold. The average element size in x- and y-direction is 14 mm. A linear interpolation function is used for both types of elements. The analysis is for thermal simulation without deformation simulation, and therefore, shear locking is not a concern in this study.

The analysis was performed with two steps: AM process simulation and service loading simulation. The purpose of the first step (AM process) is to assign the directionality of the anisotropic material properties in every element. The fibers in a printed bead are highly aligned along the deposition direction, and therefore, the anisotropic thermal properties and mechanical properties of the printed bead have a directionality along the deposition direction. The toolpath direction varies location by location in the entire printed part, as shown in Figure 2. Therefore, in the FEA model, the directionality of the anisotropic material properties of each element should be assigned based on the local toolpath direction. During the AM process simulation in Abaqus, the local toolpath directions are assigned in the FEA elements. The directionality information is transferred to the next step simulation.

Table 2: Coefficients used in the thermal simulation

Constitutive Relation	Coefficient	Value	Unit
Conduction	κ_1	1.472	W/(m·K)
	κ_2	1.287	W/(m·K)
	κ_3	0.4528	W/(m·K)
Convection	h	5.0	W/(m^2·K)
Radiation	ϵ	0.9	dimensionless

The second step is a service loading simulation. The printed mold will be placed on a heated platen of a hydraulic compression press at ORNL. The temperature of the mold will gradually increase and reach a steady state. The goal of the service loading simulation is to predict the surface temperature of the mold at a steady state. The prediction was performed via a thermal FEA simulation with the following three constitutive relations: thermal conduction, thermal convection, thermal radiation. For thermal conduction, the three-dimensional Fourier's law was used with the orthotropic conductivity coefficients ($\kappa_1, \kappa_2, \kappa_3$). For thermal convection, Newton's law of cooling was used with the convection coefficient (h). For thermal radiation, the Stefan-Boltzmann law was used with the emissivity coefficient (ϵ). The coefficients are listed in Table 2.

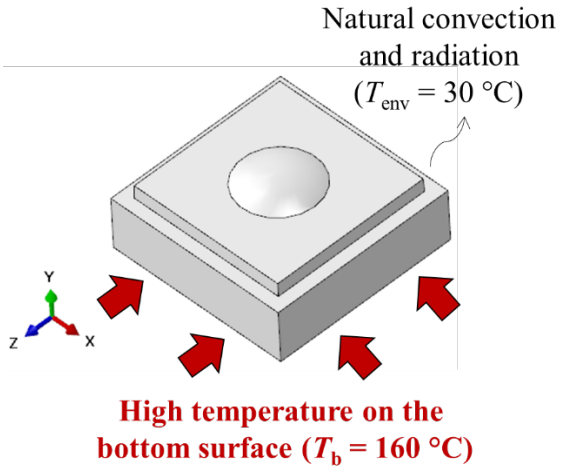


Figure 3: Boundary conditions for service load simulation (thermal simulation)

The boundary conditions are shown in Figure 3. The environment temperature was set to 30 °C, and the mold initially had a uniform temperature of 30 °C. The bottom surface temperature was set to 160 °C throughout the simulation. The convection and radiation were applied to the surface of the mold except for the bottom surface. The convection and radiation from the bottom surface were not considered. As the simulation proceeded, the temperature increased from the bottom of the mold, and the heat gradually propagated to the top surface of the mold.

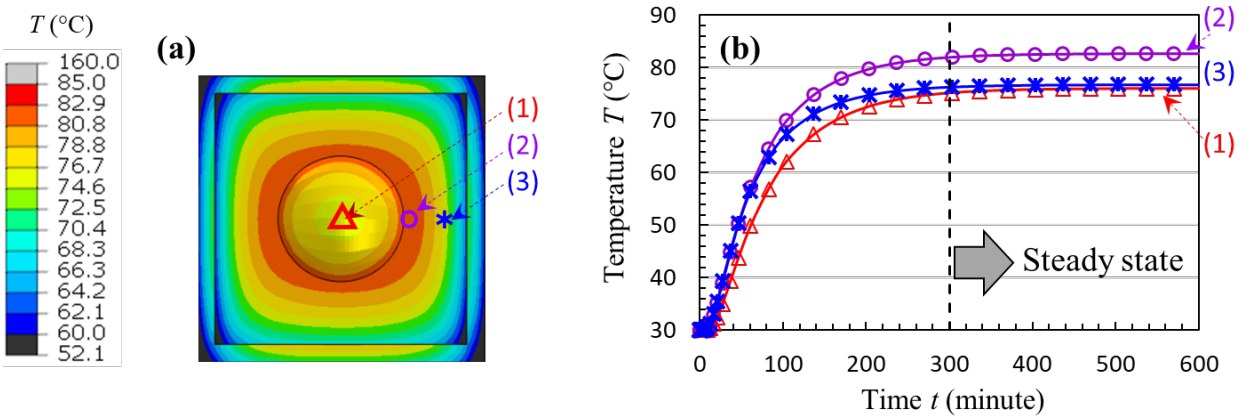


Figure 4: (a) Temperature field of the top surface at t = 600 minutes for the mold with 0°/90° infill lines and 3 perimeter lines, (b) Temperature history of the three locations indicated in Fig. (a). The temperature reached a steady state at t = 300 minutes.

Because of the heat loss via convection and radiation from the surface of the mold, the increase of the temperature slowed down and reached a steady state. Figure 4(a) shows the temperature field of the top surface at t = 600 minutes for the mold with 0°/90° infill lines and 3 perimeter lines. Three locations along the center vertical line were picked: (1) Center of the dome indicated in red '△', (2) A concave point at the interface line between the dome surface and the flat surface which is indicated in purple '◯', (3) A point further away from the center which is indicated in blue '✱'. Figure 4(b) shows the temperature history of these three locations. The temperature increased rapidly up to t = 150 ~ 200 minutes and reached a steady-state at t = 300 minutes.

The high temperature near the circular interface line between the dome surface and top flat surface may be attributed to the following reasons: (1) The center area has high temperature because of the heat loss on the surfaces at the four sides of the mold. The dome surface is further from the bottom surface (heat source) when compared to the top flat surface. Hence the conduction to the dome surface is less effective when compared to the conduction to the top flat surface. Therefore, a large area near the center has a high temperature except for the dome surface. (2) The concave surface has high temperature as compared to the convex surface because the ratio of surface area to the volume on a concave area is smaller than the ratio on a convex area.

We have performed the thermal simulations for the three molds, as shown in Figure 2, and the temperature fields of the top surfaces from the three molds are shown in Figure 5.

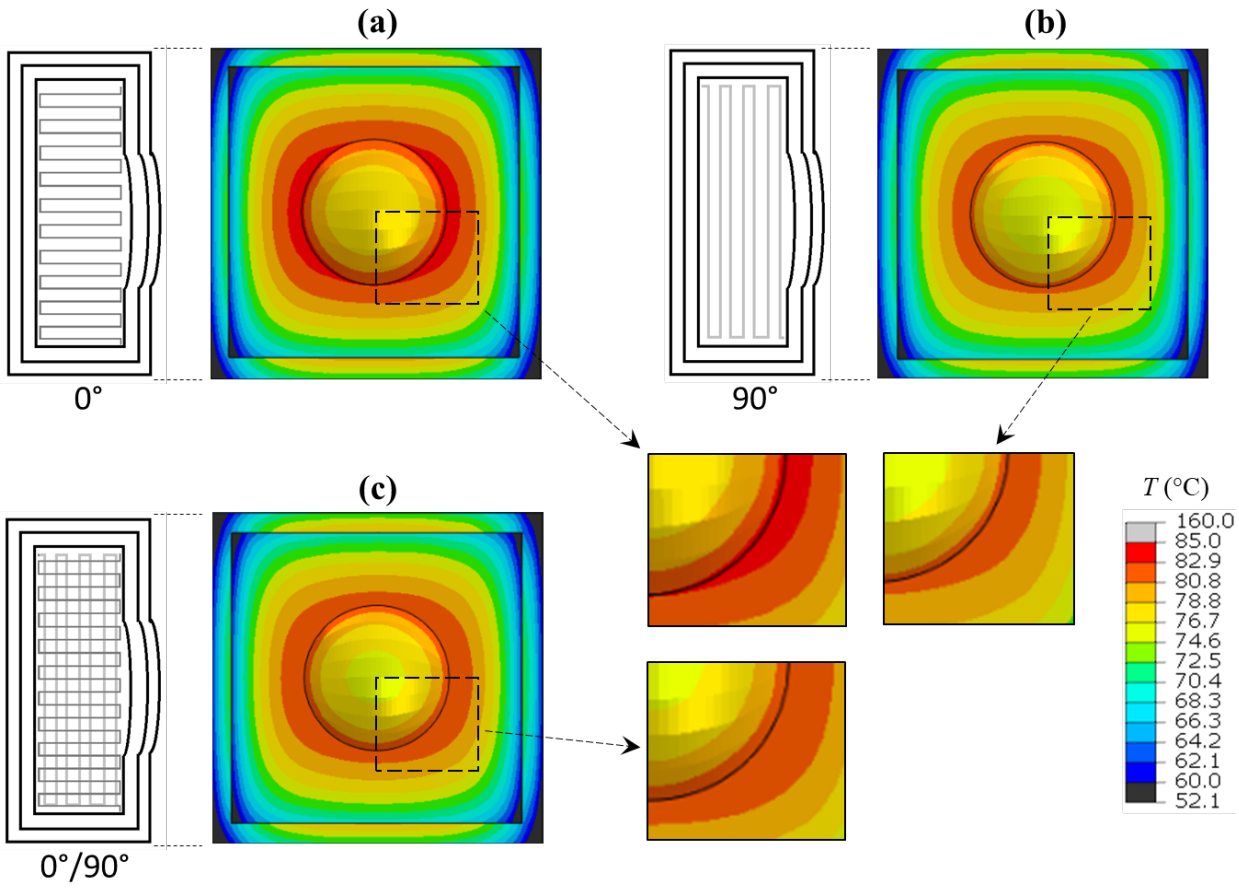


Figure 5: Temperature field of the top surface of the three molds. (a) Mold with 0° infill, (b) Mold with 90° infill, (c) Mold with 0°/90° infill.

At the interface line between the dome surface and the top flat surface, the mold with 0° infill has the highest temperature (83.9 °C), and the mold with 90° infill has the lowest temperature (82.2°C). The temperature of the mold with 0°/90° infill is in between the temperatures (82.8 °C) of 0° infill mold and 90° infill mold. Overall, the temperature of the three molds has similar profiles. The average temperatures on the surface of the interest are 79.3 °C, 77.7 °C, and 78.4 °C for 0° infill, 90° infill, and 0°/90° infill molds, respectively. The location of the peak temperature and the surface of interest is shown in Figure 6(a). Figure 6(b) shows the average temperatures of the surface of interest and the peak temperatures for the three molds with 0° infill, 90° infill, and 0/90° infill. The temperature difference between the three molds is attributed to the infill directions. An extruded material has highly aligned fibers along the deposition direction, and therefore, the conductivity along the deposition direction is higher than the conductivity in other directions. Heat transfer in the mold is mainly in the direction from the bottom surface of the mold to the top surface of the mold. If the infill direction is parallel to the heat transfer direction (0° infill), then due to the high conductivity along the heat transfer direction, the top surface holds high temperature. If the infill direction is perpendicular to the heat transfer (i.e 90° infill), then due to the low conductivity along the heat transfer direction, the top surface has low temperature.

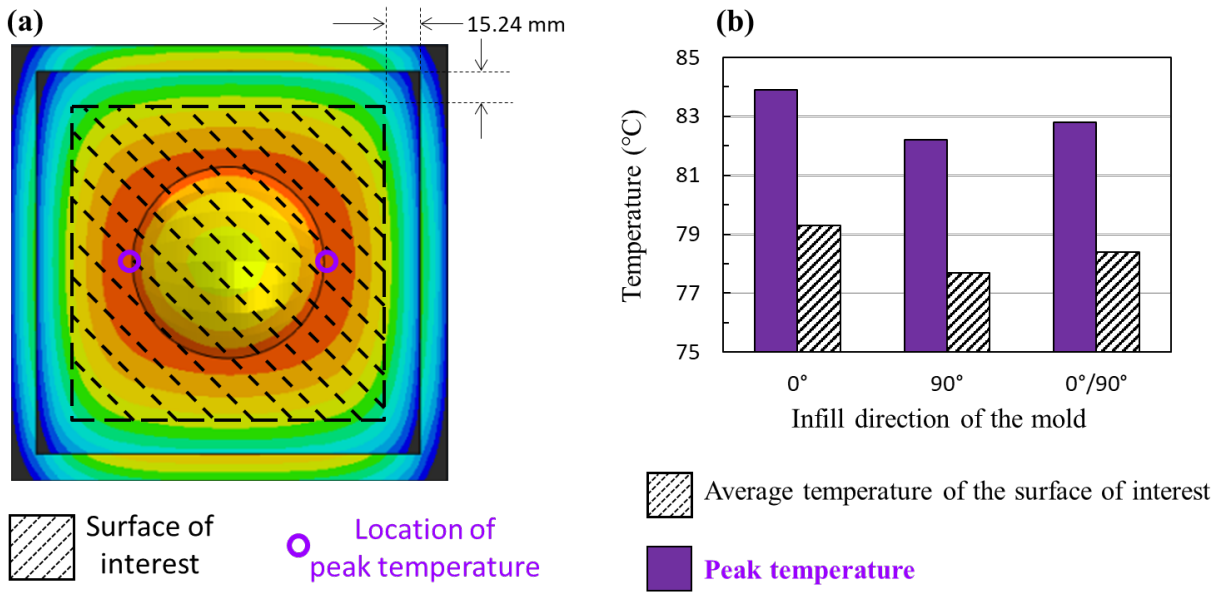


Figure 6: (a) Surface of interest (shaded area) and the location of peak temperature (purple circle) (b) Average temperatures of the surface of interest and the peak temperatures of the three molds with 0° infill, 90° infill, and 0/90° infill.

It should be noted that the current simulations have the following limitations. First, the simulation considers only the heat transfer behavior in the mold and ignores the mechanical deformation. Because the bottom surface of the mold has a high temperature (T = 160 °C) than the top surface (T = 65 - 85 °C), the thermal expansion at the bottom surface will be more significant than the thermal expansion at the top surface, which will result in warpage of the mold. The warpage of the mold will create a gap between the heated platen and the bottom surface of the mold, and the amount of the gap will be different among the three molds. Due to the gap, the bottom surface of the mold will have a non-uniform temperature distribution. Second, the simulation assumes an ideal case of infill printing in which the deposited beads have a perfect bonding. In actual large-scale printing, the deposited beads with high temperatures (extrusion temperature of 337°C), which were initially bonded to each other, might get separated as they shrink during cooling. The shrinkage of the printed beads can create a gap between infill lines, which can decrease the conductivity across the infill lines. The limitations addressed above should be considered in the simulation when we print actual molds in BAAM.

5. SUMMARY

The effect of infill pattern in AM produced molds is studied by considering the effect of CF orientation and its thermal expansion at higher temperature. The thermal conduction of the 50CF-PPS EDF-AM sample was higher in X-direction when compared with other directions (Y – and Z – direction). It was observed that the conductivity has a linear direct co-relation with temperature. FEA model was developed to understand the effect of infill pattern (0°, 90°, and 0°/90°) on the heat conduction when EDF-AM fabricated mold was placed on the heated platen. The average surface temperature of the mold was highest in 0° (79.3 °C) > 0°/90° (78.4 °C) > 90° (77.7 °C) because CFs were highly aligned along the deposition direction. The model was developed with

some limitations/assumptions; therefore, the experimental validation of the model is under development.

ACKNOWLEDGEMENT

Research sponsored by the U.S. Department of Energy, Office of Energy Efficiency and Renewable Energy, Industrial Technologies Program, under contract DE-AC05-00OR22725 with UT-Battelle, LLC.

REFERENCE

1. P. Chesser, B. Post, A. Roschli, C. Carnal, R. Lind, M. Borish, and L.J.A.M. Love, *Extrusion control for high quality printing on Big Area Additive Manufacturing (BAAM) systems.* 2019. **28**: p. 445-455.
2. B.S. Richardson, L.J. Love, P.C. Chesser, J. Miller, and A. McCalip, *Enabling Technologies for Medium Additive Manufacturing (MAAM)*. Oak Ridge National Lab.(ORNL), Oak Ridge, TN (United States). 2018.
3. M. Smith, S. Kim, A. Lambert, M. Walde, J. Lindahl, K. Mungale, . . . , and V. Kunc. *Maximizing the Performance of a 3D Printed Heat Sink by Accounting for Anisotropic Thermal Conductivity During Filament Deposition*. in *2019 18th IEEE Intersociety Conference on Thermal and Thermomechanical Phenomena in Electronic Systems (ITherm)*. 2019. IEEE.
4. Y. Jia, H. He, Y. Geng, B. Huang, X.J.C.S. Peng, and Technology, *High through-plane thermal conductivity of polymer based product with vertical alignment of graphite flakes achieved via 3D printing.* 2017. **145**: p. 55-61.
5. E. Barocio, B. Brenken, A. Favaloro, and R. Pipes. *Extrusion deposition additive manufacturing of composite molds for high-temperature applications*. in *Proceedings of the Int. SAMPE Tech. Conf., Seattle, WA, USA*. 2017.
6. V. Kunc, J. Lindahl, R. Dinwiddie, B. Post, L. Love, M. Matlack, . . . , and A. Hassen. *Investigation of in-autoclave additive manufacturing composite tooling*. in *CAMX Conference, Anaheim, CA*. 2016.
7. A.A. Hassen, J. Lindahl, X. Chen, B. Post, L. Love, and V. Kunc. *Additive manufacturing of composite tooling using high temperature thermoplastic materials*. in *SAMPE Conference Proceedings, Long Beach, CA, May*. 2016.
8. S. Kim, *An integrated design approach for infill patterning of fused deposition modeling and its application to an airfoil*. Oak Ridge National Lab.(ORNL), Oak Ridge, TN (United States). 2017.
9. S.E. Gustafsson, E. Karawacki, and M.N.J.J.o.A.P. Khan, *Determination of the thermal ‐ conductivity tensor and the heat capacity of insulating solids with the transient hot ‐ strip method.* 1981. **52**(4): p. 2596-2600.
10. V.K. Ralph B. Dinwiddie, John M. Lindahl, Seokpum Kim, Pritesh Yeole, and L.J.L. Chad Duty, Ahmed Arabi Hassen, *Specific heat capacity and anisotropic thermal conductivity of additively manufactured carbon-fiber-reinforced thermoplastics; abs + 20% cf, pps + 50% cf and ppsu + 25% cf.* . 2020: Journal of Composite Science and Technology - Under Review.